

# Time-Domain Raman Measurement of Molecular Submonolayers by Time-Resolved Reflection Spectroscopy

Satoru Fujiyoshi, Taka-aki Ishibashi,\* and Hiroshi Onishi

Surface Chemistry Laboratory, Kanagawa Academy of Science and Technology (KAST), KSP East 404, 3-2-1 Sakado, Takatsu, Kawasaki 213-0012, Japan, Core Research for Evolutional Science and Technology, Japan Science and Technology Agency, 4-1-8 Honmachi, Kawaguchi 332-0012, Japan

Received: October 27, 2003; In Final Form: November 27, 2003

Femtosecond time-resolved photoinduced reflectance change was measured on a spin-coated dye (cresyl violet) of submonolayer coverage ( $4 \times 10^{13} \text{ cm}^{-2}$ ) on a fused silica substrate. We found that the sensitivity of the reflection measurement was much higher than that of the absorption measurement for thin monolayers of dye. A prominent beating structure due to vibrational coherence of the dye was observed on the time-resolved reflection signal. A vibrational spectrum of the dye at submonolayer coverage, which corresponded to its resonance Raman spectrum, was obtained in the range 0–800  $\text{cm}^{-1}$  by a Fourier transform analysis of the reflection signal.

## 1. Introduction

Molecular monolayers have been attracting much attention because of their various applications to chemical and biological sensors, lubricators, molecular electronic devices, etc.<sup>1,2</sup> Vibrational spectroscopy is a useful tool for the characterization of molecular thin films because it provides information about identification of molecules as well as their structures. In particular, Raman spectroscopy is an attractive method to investigate a variety of interfaces because it can be carried out with only visible light. It can be applied to interfaces irrespective of its surrounding; a vacuum, high pressure gases, liquid, solids, etc., as long as the interfaces are accessible by the probe and signal lights. However, Raman scattered light is inherently weak; therefore it is difficult to obtain Raman spectra of thin films of a monolayer level thickness without recourse to signal enhancement techniques such as surface enhanced Raman scattering (SERS)<sup>3,4</sup> and resonance Raman scattering.<sup>5</sup> These enhancements have their own limitation: the SERS effect can be only expected for thin films on roughened surfaces of some metals, and a resonance Raman measurement is sometimes impossible due to strong luminescence from target molecules and impurities.

An alternative method of obtaining Raman spectra is to measure the temporal optical response of samples after the photoexcitation with a femtosecond time-resolution.<sup>6</sup> A vibrational spectrum can be obtained by a Fourier transform (FT) analysis of the beat structure (vibrational coherence) of the response.<sup>7,8</sup> This method has been established as a method for bulk analysis but has not yet been applied to thin films of a monolayer level thickness. Usually, a time-resolved measurement is performed for the transmitted probe light. In this case, the signal from the substrate is so strong that the signal from the target thin film is difficult to obtain with a good signal-to-noise-ratio. We found that this obstacle is surmountable by measuring the reflected probe light for a film thinner than the probe light wavelength. The signal of the thin film is emphasized

in comparison with that of the substrate on the temporal response of the reflected probe. In this paper, we present the first observation of vibrational coherences of cresyl violet adsorbed at submonolayer coverage on a fused silica by time-resolved reflection measurements. By the FT analysis of the observed coherences, we obtained the vibrational spectra of the submonolayer of cresyl violet in the range 0–800  $\text{cm}^{-1}$ .

## 2. Experimental Section

A noncollinear optical parametric amplifier (TOPAS-white, Quantronix) pumped by a femtosecond Ti:sapphire regenerative amplifier (Hurricane, Spectra Physics) was used as a light source. The wavelength of the output was tunable in the range 510–700 nm. The output (1 kHz) was divided into three parts used as pump, probe, and reference pulses. The pump and probe pulses were crossed on the sample surface at an angle of 2°. The incident angle of the probe pulse was 8–10° with respect to the surface normal. The polarizations of the pump and probe pulses were s-polarization. The pump and probe energies were 0.2 and 0.02  $\mu\text{J}$ , respectively, and their spot diameter at the sample position was 0.1 mm. The intensities of the probe and reference pulses were detected by photodiodes coupled with current preamplifiers, and the difference of the photodiode outputs was amplified with a differential amplifier. The differentially amplified output was gated with a boxcar integrator, A/D converted, and sent to a personal computer on a pulse-to-pulse basis. The pump pulse was modulated at 500 Hz with a synchronous mechanical chopper. The signals with pump on and off were separately accumulated on the computer, and the pump induced reflectance or transmittance change was calculated. The instrumental response at the sample position was determined as the intensity autocorrelation between the pump and probe pulses using second harmonic generation in a 50- $\mu\text{m}$ -thick  $\beta\text{-BaB}_2\text{O}_4$  crystal. The full width at half-maximum (fwhm) of the instrumental response was typically 23 fs.

Cresyl violet (Exciton) and HPLC-grade ethanol (Wako Pure Chemical) were used without further purification. For the

\* To whom the correspondence should be addressed. E-mail: ti@net.ksp.or.jp.

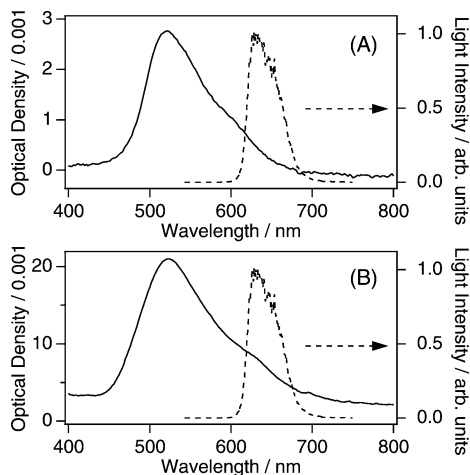


**Figure 1.** Steady-state absorption spectra of cresyl violet on fused silica (solid line) and spectra of a light source for time-resolved measurements (dotted line). The surface molecular densities of the dye were  $4 \times 10^{13} \text{ cm}^{-2}$  (A) and  $1 \times 10^{15} \text{ cm}^{-2}$  (B).

transmission measurements, 1-mm-thick fused silica was used as a substrate. For the reflection measurements, 5-mm-thick wedged fused silica was used as a substrate. The samples were prepared by spin-coating ethanol solutions of cresyl violet on the substrates at 2000 rpm for 1 min. For the evaluation of the surface molecular density of the sample, we redissolved dye molecules on a substrate in solvent of a known volume and estimated the number of the molecules on the substrates by absorption spectra of the solution. The number density of the molecules thus estimated was  $4 \times 10^{13}$  and  $1 \times 10^{15} \text{ cm}^{-2}$  for the substrates spin-coated with 0.1 and 4 mM ethanol solutions, respectively. The number density of  $4 \times 10^{13} \text{ cm}^{-2}$  corresponds to 0.4 monolayer, if the area of the molecule is assumed to be  $1 \text{ nm}^2$ .

### 3. Results and Discussion

Figure 1 shows the steady-state absorption spectra of cresyl violet on fused silica whose surface molecular densities were  $4 \times 10^{13} \text{ cm}^{-2}$  (A) and  $1 \times 10^{15} \text{ cm}^{-2}$  (B). Both absorption spectra have a peak at 520 nm and a shoulder at 600 nm. The absorption band of the thinner sample (A) was slightly narrower than that of the thicker sample (B). The spectrum of a light source for time-resolved measurements is also shown as a broken curve in this figure. We tuned the excitation wavelength to the red-edge of the absorption.

Photoinduced transmittance and reflectance changes were observed as a function of the delay time between the pump and probe pulses. The time-resolved transmittance of cresyl violet on fused silica (a) and the substrate (b) are shown in Figure 2. Around the time origin, a spike-like response was observed in both signals. The spike-like response was attributed to the substrate because it appeared irrespective of the existence of the dye. The response was assigned to the nonresonant electronic response.<sup>8–10</sup> After the depletion of the spike-like response, we observed a long-lived component due to the transient gain of cresyl violet in Figure 2a. The signal of the dye, expanded by a factor of 6, is depicted in Figure 2c by subtracting (b) from (a). The peak intensity of the signal of the dye is 7 times smaller than that of the signal due to the substrate. In contrast to the transmission signal, the time-resolved reflection signal of the dye layer (Figure 2d) was dominated by the response of cresyl violet. The peak intensity of the response of the dye (Figure

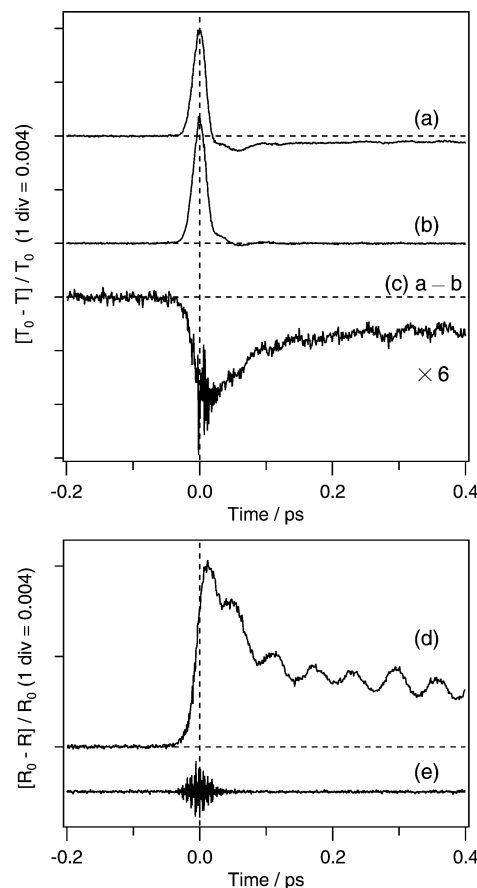


**Figure 2.** Time-resolved transmission signals of cresyl violet adsorbed on fused silica: (a) spin-coated film of the dye; (b) silica substrate; (c) subtracted trace (a) – (b), which is expanded by a factor of 6. Time-resolved reflection signals of cresyl violet on fused silica: (d) spin-coated film of the dye; (e) silica substrate. The surface molecular densities were  $1 \times 10^{15} \text{ cm}^{-2}$ . The interval of data points was 1 fs. Each data point was obtained by averaging over 6000 probe pulses.

2d) was 8 times larger than that of the signal of the substrate<sup>11</sup> (Figure 2e). The result clearly shows that the signal of the molecular thin film is emphasized, compared with that of the substrate (bulk) in the reflection arrangement.

The signal-to-noise ratio of the reflection signal of cresyl violet (Figure 2d) is significantly better than that of its transmission signal (Figure 2c) because the amplitude of the reflectance change of the dye ( $\Delta R = [R_0 - R]/R_0$ ) is  $\sim 6$  times larger than that of its transmittance change ( $\Delta T = [T_0 - T]/T_0$ ). Here, we discuss the origin of the difference. Total intensities of the transmitted probe light  $I_T$  and the reflected probe light  $I_R$  can be expressed as

$$I_T = |E_s e^{i\theta} + E_0|^2 \quad I_R = |E_s e^{i\theta} + E_{R_0} e^{i\phi}|^2 \quad (1)$$

where  $E_s$  is the amplitude of the electric field of the signal obtained from the dye;  $E_0$  and  $E_{R_0}$  are those of the transmitted and the reflected probe lights;  $\theta$  and  $\phi$  are the phases of the electric fields of the signal and reflected probe lights with respect to that of the probe light. It is well-known that a sheet of a nonlinear polarization radiates light equally in the transmitted and reflected directions, when the thickness of the samples is thin compared with the probe wavelength.<sup>12</sup> We assume in eq 1 the same field amplitude from the dye layer for  $I_T$  and  $I_R$  because the thickness of the layer of the sample was much shorter than the probe wavelength. It is known that the phase

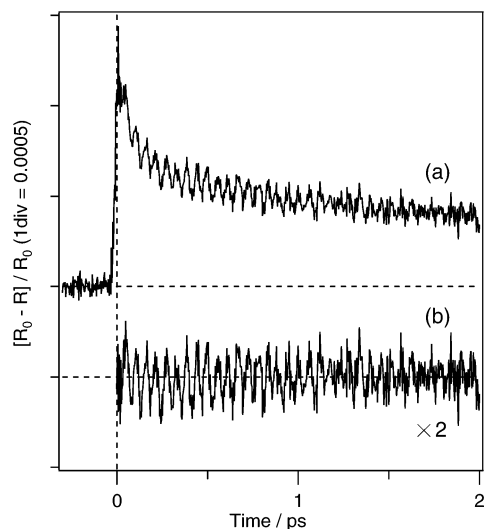


**Figure 3.** (a) Time-resolved reflection signals of cresyl violet on fused silica in the range  $-0.3$  to  $+2$  ps. The surface molecular density was  $4 \times 10^{13} \text{ cm}^{-2}$ . The interval of data points was 3 fs. Each data point was obtained by averaging over 6600 probe pulses. (b) Subtracted vibrational coherence, which is vertically expanded by a factor of 2.

of an s-polarized electric field reflected at an air–substrate boundary is  $\pi$  with respect to that of the incident electric field ( $\phi = \pi$ ). Assuming the signal fields are much smaller than the probe fields ( $|E_s| \ll |E_0|$  and  $|E_{R_0}|$ ), the changes  $\Delta T$  and  $\Delta R$  approximated as

$$\Delta T = -2(E_s/E_0) \cos \theta \quad \Delta R = 2(E_s/E_{R_0}) \cos \theta \quad (2)$$

and then the ratio of  $\Delta R$  to  $\Delta T$  becomes

$$\Delta R/\Delta T = -(E_0/E_{R_0}) \quad (3)$$

We determined the ratio  $|E_0/E_{R_0}|$  to be 5 by measuring the intensities of the transmitted and reflected probe lights. The number is consistent with the observed ratio  $\Delta R/\Delta T$  of  $-6$ . Thus, the advantage of reflection measurements over transmittance measurements is rationalized for the case of thin monolayers of dye on transparent substrates.

Figure 3a shows the time-resolved reflection signals of cresyl violet at submonolayer coverage ( $4 \times 10^{13} \text{ cm}^{-2}$ ) up to the delay time of 2 ps. An oscillatory component due to vibrational coherence was distinctly observed on a rise-and-decay nonoscillatory component. The nonoscillatory component was attributed to the excited-state dynamics of cresyl violet. To analyze the vibrational coherence, the nonoscillatory component was subtracted from the total signal. For the subtraction, the nonoscillatory component was able to fit the sum of the exponential functions convoluted with the instrumental response. The extracted oscillatory component is depicted in Figure 3b. Time constants of  $\tau_1 = 73$  fs,  $\tau_2 = 0.87$  ps,  $\tau_3 = 11$  ps,  $\tau_4 > 100$  ps with respective amplitudes of  $A_1 = 0.44$ ,  $A_2 = 0.24$ ,  $A_3 = 0.29$ ,  $A_4 = 0.02$  were evaluated. In this fitting analysis, some of the parameters ( $\tau_3$ ,  $\tau_4$ ,  $A_3$ , and  $A_4$ ) were predetermined using the signal of 3–100 ps. Time constants  $\tau_3$  and  $\tau_4$  were attributed to the vibrational cooling time of excited-state cresyl violet<sup>13,14</sup> and the nanosecond lifetime of the excited-state dye,<sup>15</sup> respectively. The assignments of the two remaining fast components ( $\tau_1$  and  $\tau_2$ ) are not definite. Ultrafast responses with decay constants similar to  $\tau_1$  and  $\tau_2$  have been observed and assigned to the solvation process of dye molecules.<sup>14,16–20</sup> On the basis

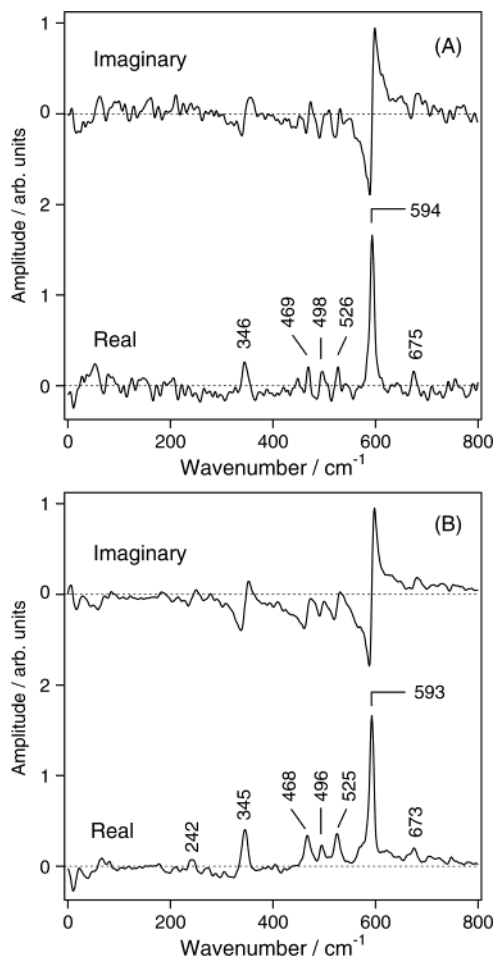


**Figure 4.** Real and imaginary parts of Fourier transform spectra of the time-resolved reflection signals. The surface molecular densities were  $4 \times 10^{13} \text{ cm}^{-2}$  (A) and  $1 \times 10^{15} \text{ cm}^{-2}$  (B).

of the previous works, we tentatively assigned  $\tau_1$  and  $\tau_2$  components to the relaxation process between the excited and neighboring dye molecules.

To represent the vibrational coherences (Figure 3b) in the frequency domain, an FT analysis of the oscillatory component was performed. We used the subtracted signal in the range 0–5 ps for the FT analysis. Before the FT analysis, we multiplied the oscillatory component by a window function, which is a Gaussian function having a fwhm of 4.5 ps, and we added zero data points from 5 to 25 ps to decrease the data-point interval in the frequency domain. Figure 4A shows the imaginary and real parts of the FT spectrum in the range 0–800  $\text{cm}^{-1}$  for cresyl violet at the submonolayer coverage ( $4 \times 10^{13} \text{ cm}^{-2}$ ). Vibrational bands in the real part had a positive, symmetric shape, whereas those in the imaginary part had dispersive shapes. The obtained band-shape characteristic means that the observed vibrational coherence, which corresponds to the imaginary part of the third-order nonlinear polarization,<sup>8</sup> is approximately expressed as a sum of cosine functions ( $R_{\text{obs}}(t) \sim \sum A_{\text{vib}} \cos \omega_{\text{vib}} t$ ). Six peaks at 346, 469, 498, 526, 594, and 675  $\text{cm}^{-1}$  were identified in the real part of the spectrum. The frequency of the strongest band (594  $\text{cm}^{-1}$ ) coincides with ones that Joo and Albrecht measured on solutions of cresyl violet by time-resolved transmission and resonance Raman spectroscopies.<sup>21</sup> The resonance Raman spectrum of cresyl violet in water had the strongest band at 593  $\text{cm}^{-1}$  and its intensity pattern is similar to the real part spectrum of ours. As for the time-resolved measurement, cresyl violet solution in ethylene glycol presented a periodic

oscillation corresponding to the frequency of ca.  $590\text{ cm}^{-1}$ . The oscillation amplitude decayed with two time constants of 0.19 and 1.3 ps. They assigned the fast and slow decaying components to the vibrational coherences of the electronically excited and ground states of the dye, respectively. The present measurement (Figure 3b) shows no fast decaying oscillation corresponding to the 0.19-ps component. Taking account of the results on the solutions of cresyl violet, we conclude that the observed vibrational coherence is attributed to the vibration of the ground state of cresyl violet. The frequencies of the six bands (Figure 4A) are in excellent agreement with those of the bands obtained from the real part of the spectrum of the thicker sample (Figure 4B). This agreement can best be understood by either or both of the following two explanations. One is that the molecular aggregations of the thicker and thinner samples were very similar, forming the islandlike aggregation in the thinner samples. The other is that the intermolecular interaction and interaction between the dye and the substrate were too small to affect molecular vibrations.

The present results clearly show that our apparatus is capable of measuring Raman spectra of thin films of dye molecules in the range  $0\text{--}800\text{ cm}^{-1}$ . The submonolayer sensitivity of the method was successfully demonstrated. It should be noted that the disturbance of the fluorescence was negligibly small in our measurement although the excitation wavelength was set near the peak of the fluorescence of cresyl violet. One of the advantages of this method over ordinary frequency-domain spontaneous Raman spectroscopy is that it is applicable to low frequency vibrations of highly fluorescent samples.

**Acknowledgment.** We thank Prof. Masahiro Kotani and Mr. Hiroyuki Kobayashi of Gakushuin University for advice in sample preparations. This work was supported by Grant-in-Aids for Scientific Research from the Ministry of Education, Culture, Sports, Science Technology of Japan (No. 13555008, 14654108).

## References and Notes

- (1) Ulman, A. *An Introduction to Ultrathin Organic Films from Langmuir–Blodgett to Self-Assembly*; Academic Press: San Diego, CA, 1991.
- (2) Adams, D. M.; Brus, L.; Chidsey, C. E. D.; Creager, S.; Creutz, C.; Kagan, C. R.; Kamat, P. V.; Lieberman, M.; Lindsay, S.; Marcus, R. A.; Metzger, R. M.; Michel-Beyerle, M. E.; Müller, J. R.; Newton, M. D.; Rolison, D. R.; Sankey, O.; Schanze, K. S.; Yardley, J.; Zhu, X. *J. Phys. Chem. B* **2003**, *107*, 6668.
- (3) Otto, A.; Mrozek, I.; Grabhorn, H.; Akemann, W. *J. Phys.: Condens. Matter* **1992**, *4*, 1143.
- (4) Campion, A.; Kambhampati, P. *Chem. Soc. Rev.* **1998**, *27*, 241.
- (5) Hamaguchi, H. In *Advances in Infrared and Raman Spectroscopy*; Clark, R. J. H., Hester, R. E., Eds.; Wiley: Heyden, 1985; Vol. 12, p 273.
- (6) Dhar, L.; Rogers, J. A.; Nelson, K. A. *Chem. Rev.* **1994**, *94*, 157.
- (7) Cho, M.; Du, M.; Scherer, N. F.; Fleming, G. R.; Mukamel, S. *J. Chem. Phys.* **1993**, *99*, 2410.
- (8) Ziegler, L. D.; Fan, R.; Desrosiers, A. E.; Scherer, N. F. *J. Chem. Phys.* **1994**, *100*, 1823.
- (9) Goodno, G. D.; Miller, R. J. D. *J. Phys. Chem. A* **1999**, *103*, 10619.
- (10) Khalil, M.; Demirodöven, N.; Golonzka, O.; Fecko, C. J.; Tokmakoff, A. *J. Phys. Chem. A* **2000**, *104*, 5711.
- (11) The temporal behavior of the response of the substrate (Figure 2e) is apparently different from that of the electronic response observed in the time-resolved absorption measurements (Figure 2b). The temporal behavior (Figure 2e) probably reflects the optical interference between the pump and probe pulses. This type of interference appeared when the incident angle of the probe light was close to the surface normal of the substrate.
- (12) Bloembergen, N.; Pershan, P. S. *Phys. Rev.* **1962**, *128*, 606.
- (13) Iwata, K.; Hamaguchi, H. *J. Phys. Chem. A* **1997**, *101*, 632.
- (14) Fujiyoshi, S.; Takeuchi, S.; Tahara, T. *J. Phys. Chem. A* **2003**, *107*, 494.
- (15) Anfinrud, P.; Crackel, R. L.; Struve, W. S. *J. Phys. Chem.* **1984**, *88*, 5873.
- (16) Walker, G. C.; Jarzeba, W.; Kang, T. J.; Johnson, A. E.; Barbara, P. F. *J. Opt. Soc. Am. B* **1990**, *7*, 1521.
- (17) Joo, T.; Jia, Y.; Yu, J.-Y.; Lang, M. J.; Fleming, G. R. *J. Chem. Phys.* **1996**, *104*, 6089.
- (18) Passino, S. A.; Nagasawa, Y.; Joo, T.; Fleming, G. R. *J. Phys. Chem. A* **1997**, *101*, 725.
- (19) Shang, X.; Benderskii, A. V.; Eisinger, K. B. *J. Phys. Chem. B* **2001**, *105*, 11578.
- (20) Benderskii, A. V.; Eisinger, K. B. *J. Phys. Chem. B* **2001**, *105*, 6698.
- (21) Joo, T.; Albrecht, A. C. *Chem. Phys.* **1993**, *173*, 17.